NEUROSCIENCE

Synapse-specific representation of the identity of overlapping memory engrams

Kareem Abdou[1,2]*, Mohammad Shehata[1,2]*†‡, Kiriko Choko[1,2], Hirofumi Nishizono[2,3], Mina Matsuo[3], Shin-ichi Muramatsu[4,5], Kaoru Inokuchi[1,2]§

Memories are integrated into interconnected networks; nevertheless, each memory has its own identity. How the brain defines specific memory identity out of intermingled memories stored in a shared cell ensemble has remained elusive. We found that after complete retrograde amnesia of auditory fear conditioning in mice, optogenetic stimulation of the auditory inputs to the lateral amygdala failed to induce memory recall, implying that the memory engram no longer existed in that circuit. Complete amnesia of a given fear memory did not affect another linked fear memory encoded in the shared ensemble. Optogenetic potentiation or depotentiation of the plasticity at synapses specific to one memory affected the recall of only that memory. Thus, the sharing of engram cells underlies the linkage between memories, whereas synapse-specific plasticity guarantees the identity and storage of individual memories.

Memories are formed through long-term changes in synaptic efficacy, a process known as synaptic plasticity (*1*–*7*), and are stored in the brain in specific neuronal ensembles called engram cells, which are reactivated during memory retrieval (*8*–*13*). When two memories are associated, cell ensembles corresponding to each memory overlap (*14*–*19*) and are responsible for the association (*18*). Although multiple associated memories can be encoded in the overlapping population of cells, each memory has its own identity (*14*, *18*). Synaptic plasticity is essential for the retrieval, but not the storage, of associative fear memories (*5*, *20*, *21*). However, how the brain defines the identity of a particular memory amid the many memories stored in the same ensemble has been elusive.

We asked whether individual memories stored in a shared neuronal ensemble would maintain their identities and have a different fate if one memory was erased by complete retrograde amnesia. We subjected mice to auditory fear conditioning (AFC), in which a tone was associated with a foot shock. This association is mediated by synaptic plasticity between neuron terminals of the auditory cortex (AC) and the medial part of the medial geniculate nucleus (MGm) and neurons of the lateral amygdala (LA) (*22*). Two different tones, at 2 and 7 kHz, were used. Mice discriminated between the two tones and showed a freezing response only to the 7-kHz tone that was paired with shock (figs. S1 and S2). To completely erase memories, we used autophagy, which is a major protein degradation pathway wherein the autophagosome sequesters a small portion of the cytoplasm and fuses with the endosome-lysosome system to degrade the entrapped contents. Autophagy contributes to synaptic plasticity (*23*, *24*), and its induction by the peptide tat-beclin enhances destabilization of synaptic efficacy after reactivation of these synapses through the degradation of endocytosed α-amino-3-hydroxy-5-methyl-4-isoxazolepropionic acid receptors (*25*, *26*). When tat-beclin is combined with inhibition of protein synthesis after memory retrieval, complete retrograde amnesia is induced through enhanced memory destabilization and reconsolidation inhibition (*25*).

To optogenetically manipulate specific memories, we used c-Fos::tTA transgenic mice; we injected adeno-associated virus (AAV) expressing Cre recombinase under the control of tetracycline-responsive element (TRE) in combination with AAV encoding DIO-oChIEF-citrine, downstream of the human synapsin (hSyn) 1 promoter, into the AC and MGm (both of which relay auditory information to the LA) to label the activated ensemble with a channelrhodopsin variant, oChIEF (Fig. 1, A to D, and fig. S2). Mice were trained with AFC (7-kHz tone plus shock) 2 days after doxycycline withdrawal (OFF DOX). One day later, under the ON DOX condition, the LAs of these mice were infused with phosphate-buffered saline (PBS), anisomycin, or anisomycin combined with tat-beclin (Ani+tBC) immediately after the test session (day 5). The anisomycin infusion induced partial retrograde amnesia, whereas Ani+tBC accomplished complete amnesia, with the freezing level comparable to that of nonshocked and unpaired control groups (Fig. 1E). Optogenetic activation of the axonal terminals of the AC and MGm engram cells in the LA induced fear memory recall in the PBS and anisomycin groups, which is consistent with a previous study (*21*), whereas it failed to do this in the Ani+tBC-treated mice (Fig. 1F).

To further confirm memory erasure, we tried to recover the erased memories by using optical long-term potentiation (LTP). High-frequency optical stimulation of the terminals of AC and MGm engram cells to the LA led to long-lasting potentiated field responses (fig. S3, A and B). Optical LTP allowed anisomycin-treated mice to completely recover from amnesia to the PBS group's freezing level, which was specific to the 7-kHz conditioned tone (i.e., it did not generalize to the 2-kHz tone) (Fig. 1G). In the Ani+tBC-treated mice, optical LTP failed to completely recover the fear memory; these mice showed only a slight increase in the freezing level, which was similar to that which occurred in the unpaired control group (Fig. 1G). Because the unpaired conditioning did not form an associative fear memory, this slight increase in the freezing response might be attributed to the formation of a new artificial associative memory, rather than restoration of a previously stored associative memory.

In a remote memory test, the Ani+tBC group displayed significantly lower freezing than the anisomycin or PBS groups in both natural cue and optogenetic tests, indicating that memory erasure was long-lasting and that the memory did not undergo spontaneous recovery over time (Fig. 1, H and I). The Ani+tBC-treated mice that received LTP showed light-induced freezing comparable to that of the PBS group (test 9), excluding the possibility of LA damage from Ani+tBC treatment. Furthermore, similar results were obtained when engram cells in the LA were labeled and manipulated similarly but optical (instead of tone) recall was used (fig. S4).

To examine the synaptic mechanism underlying the complete retrograde amnesia, we conducted a LTP occlusion experiment, in which artificial induction of LTP was occluded in circuits with potentiated synapses, whereas it was facilitated in circuits with unpotentiated synapses (*27*–*29*). High-frequency optical stimulation 1 day after test 1 induced LTP in the Ani+tBC group that was comparable to that in the nonshock group but significantly higher than that in the PBS and anisomycin groups (Fig. 2, A to D). Thus, synaptic plasticity was totally reset and returned to nonshock levels after complete amnesia.

This conclusion was further supported by analysis of functional connectivity. Using c-Fos::tTA/R26R::H2B-mCherry double transgenic mice (*18*), we measured the connectivity pattern between upstream and downstream engram cells after memory erasure. Engram cells in the LA were labeled with Cre-dependent mCherry, and the axonal terminals of the AC and MGm engram cells were labeled with oChIEF. The terminals were optogenetically stimulated at 10 Hz, and the number of cells that were double-positive for mCherry and c-Fos, which represented the degree of functional connectivity

[1]Department of Biochemistry, Graduate School of Medicine and Pharmaceutical Sciences, University of Toyama, Toyama 930-0194, Japan. [2]Japan Science and Technology Agency, CREST, University of Toyama, Toyama 930-0194, Japan. [3]Division of Animal Experimental Laboratory, Life Science Research Center, University of Toyama, Toyama 930-0194, Japan. [4]Division of Neurology, Department of Medicine, Jichi Medical University, Tochigi 3290498, Japan. [5]Center for Gene and Cell Therapy, The Institute of Medical Science, The University of Tokyo, Tokyo 1088639, Japan.
*These authors contributed equally to this work. †Present address: Division of Biology and Biological Engineering, California Institute of Technology, Pasadena, CA 91125, USA. ‡Present address: Mind and Brain Laboratory for Perceptual and Cognitive Processing, Toyohashi University of Technology, Toyohashi 441-8580, Japan.
§Corresponding author. Email: inokuchi@med.u-toyama.ac.jp

between upstream and downstream engram cells, was counted (Fig. 2, E to I, and fig. S7, A and B). Complete amnesia resulted in a significant decrease in the c-Fos^{+}–mCherry^{+} overlap in the Ani+tBC group in comparison with the PBS and anisomycin groups, which is consistent with the behavioral data and the total resetting of synaptic efficacy.

Considering that memories are stored in interconnected networks, and the brain can store two memories in a shared ensemble (*14*–*18*), we examined the effect of complete retrograde amnesia of one memory on another memory by using two different AFC events: a 7-kHz AFC (event 1) followed by a 2-kHz AFC (event 2) (Fig. 3). When these two events were separated by 5 hours, memory for event 2 was enhanced (fig. S5), indicating interaction between the memories

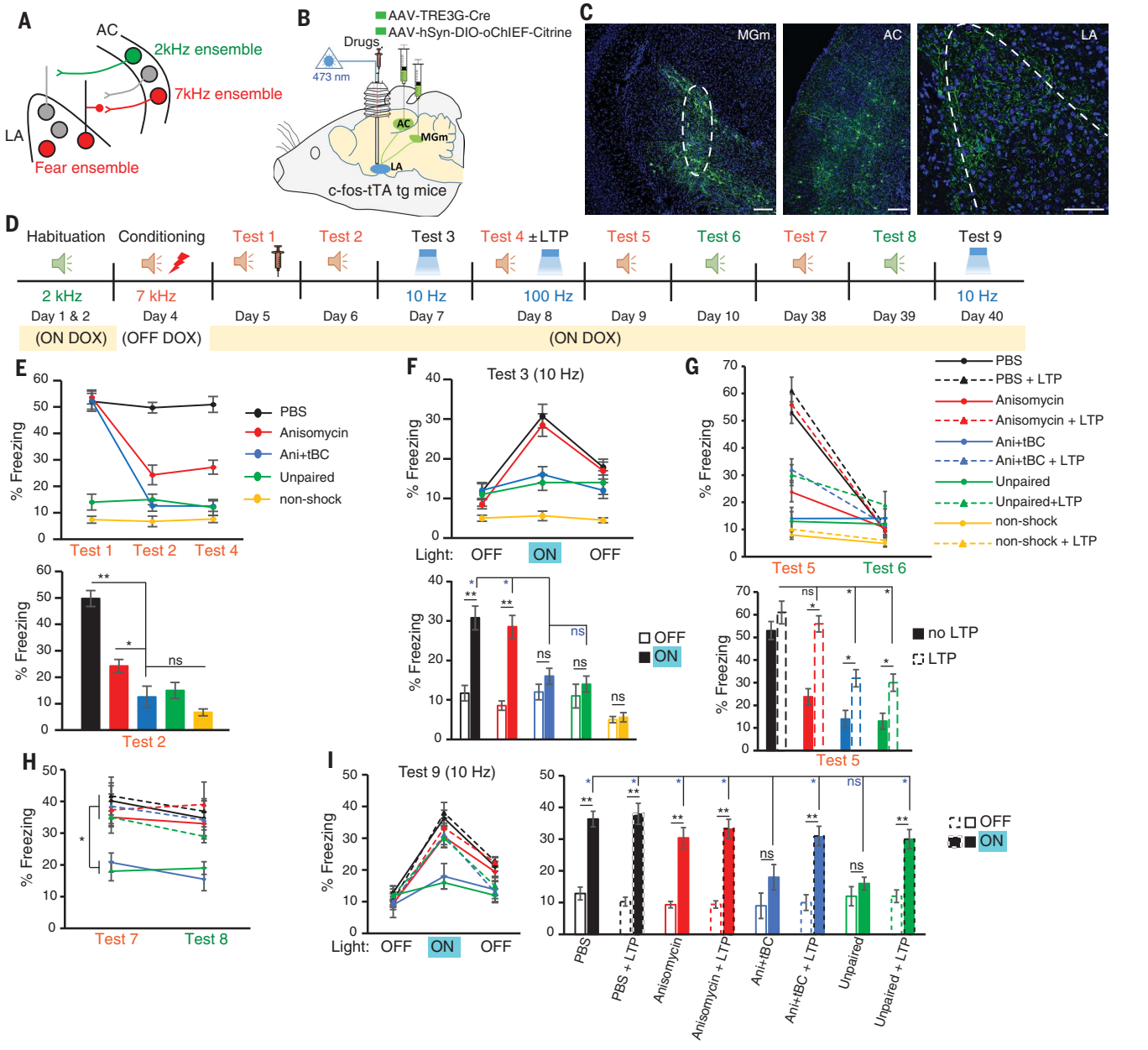

Fig. 1. Complete and long-lasting erasure of fear memory trace from AC-LA and MGm-LA engram circuits. (**A**) Model showing the ensemble responsive to the 2- and 7-kHz tones in the AC and the fear-responsive ensemble in the LA. (**B**) Labeling strategy for the AFC-responsive ensemble in the AC and MGm, using the c-Fos::tTA transgenic mice. (**C**) Expression of oChIEF in AC and MGm neurons and their axonal terminals in the LA. Dashed lines show the borders of the MGm and LA. Scale bars, 100 μm. (**D**) Design of memory engram erasure experiment. Different chambers were used for each session. (**E** to **I**) Freezing levels (percent of time) before and after drug injection (E), during 10-Hz optical stimulation (F), in response to the conditioned and neutral tones after optical LTP (G), at a remote time point (H), and during 10-Hz stimulation at a remote time point (I). n = 20 mice per group in (E) and (F) and 10 mice per group in (G) to (I). Bottom panels of (E) to (G) show statistical significance between groups during test 2 (E), during light-off and light-on epochs (F), and during test 5 (G). The right panel of (I) shows statistical significance within and between groups during test 9. Statistical comparisons were performed using one-way analysis of variance (ANOVA) [(E), (G), and (H)] and two-way ANOVA [(F) and (I)]. *P < 0.05; **P < 0.01; ns, not significant. In the bottom panels of (F), (G), and (I), the colors of the upper asterisks indicate the comparison (e.g., blue asterisks indicate a comparison with the Ani+tBC group). Data are represented as mean ± SEM. Ani, anisomycin; tBC, tat-beclin.

(*17*). The majority of the LA engram cells for event 1 (mCherry$^+$) also encoded event 2 (c-Fos$^+$), whereas the memories were encoded in two distinct populations in the AC (Fig. 3, A to E, and fig. S7, C to F). When the two memories were separated by 24 hours, they were allocated to distinct populations in both the LA and the AC.

We then used the c-Fos::tTA transgenic mice to label the neural ensembles in the AC and MGm that were activated specifically during event 1 with oChIEF (Fig. 3F and fig. S6). After 5 hours ON DOX, mice were exposed to event 2 and then divided into two groups. The first group received PBS after event 1 memory retrieval and Ani+tBC after event 2 memory retrieval (gp1), whereas the second group received the opposite treatment (gp2). In gp1, memory of event 2 was erased by Ani+tBC (test 4), whereas memory of event 1 was not affected (test 2). In contrast, in gp2, event 1 memory was erased (test 2), whereas event 2 memory was not affected (test 4; Fig. 3G). Moreover, optogenetic stimulation of the presynaptic terminals of the AC and MGm engram cells corresponding to event 1 memory induced a freezing response in gp1, but not in gp2, although in both groups, the LA neurons storing both associative memories underwent Ani+tBC treatment (Fig. 3H). These results reveal synapse-specific engram erasure and indicate that memories stored in the shared engram cells are synapse-specific and have different fates (Fig. 3I).

We then addressed the question of how each memory reserves its individual identity within the shared ensemble. We carried out a loss-of-function experiment using optical long-term depression (LTD) to depotentiate the synaptic efficacy in synapses specific for event 1 memory (fig. S3, A and C, and Fig. 4, A and B). In comparison with a control group, mice that received LTD showed impairment in event 1 memory recall, but not in event 2 memory recall (Fig. 4C). Optogenetic stimulation to the terminals of the AC and MGm ensemble of event 1 memory triggered freezing in the control group, whereas it failed to trigger freezing in the LTD group, despite the fact that event 2 memory was intact (Fig. 4D). Thus, selective depotentiation of synaptic plasticity deconstructs the specific connectivity between engram assemblies, thereby erasing one memory without disrupting the other memory in the same population of neurons.

Last, a gain-of-function experiment was performed in which both memories were erased with Ani+tBC and then optical LTP was induced

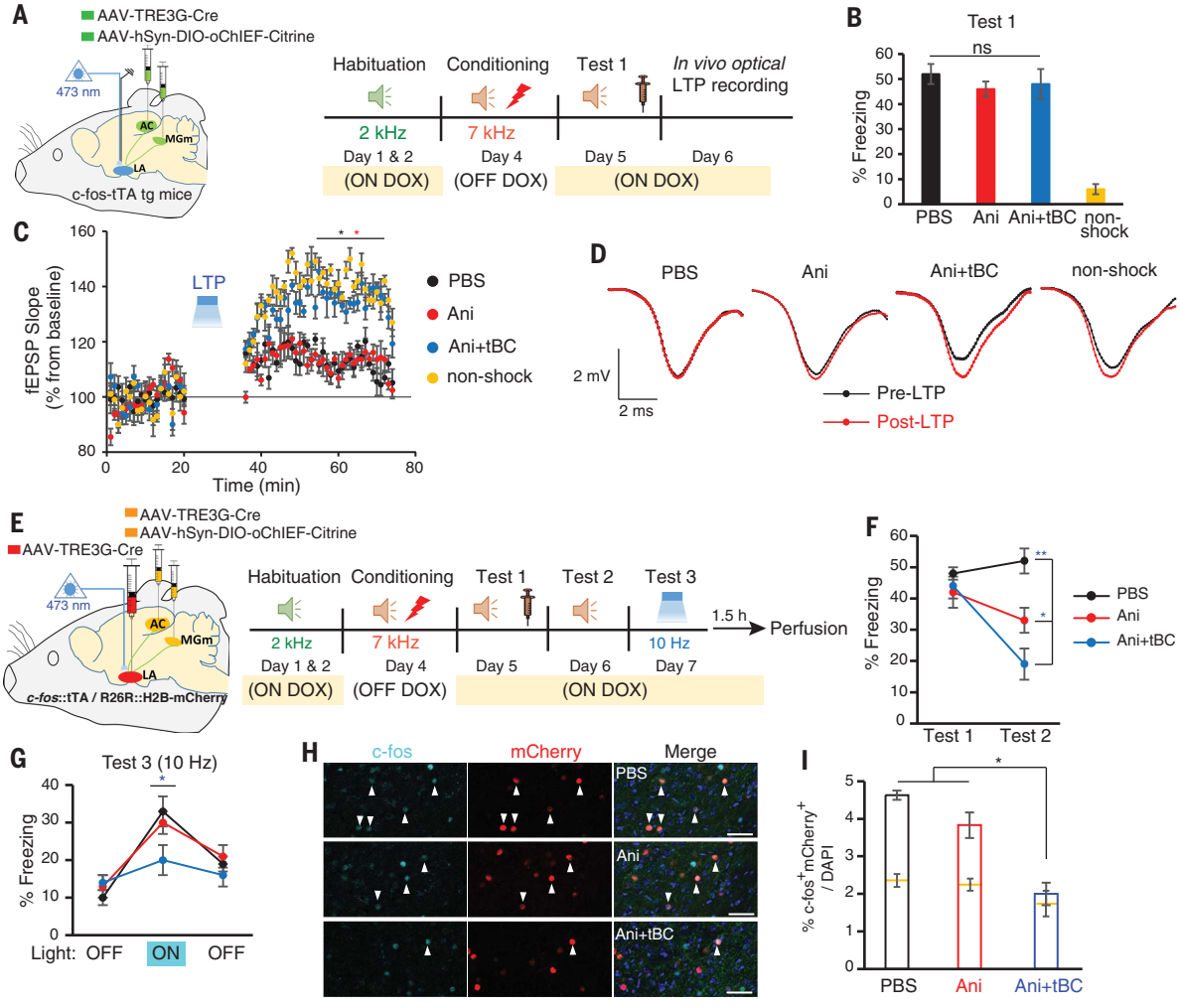

Fig. 2. Resetting of synaptic plasticity and functional connectivity between engram cell assemblies as neural correlates of complete amnesia. (**A**) Left, labeling strategy. Right, experimental design for the LTP occlusion experiment. (**B**) Freezing level during test 1. (**C**) Average of in vivo field excitatory postsynaptic potential slope (normalized to baseline) before and after LTP induction (two-way repeated-measures ANOVA; $n = 4$ mice per group). (**D**) Traces before (black) and after (red) optical LTP induction. (**E**) Left, labeling of engram cell assemblies in the AC, MGm, and LA using double transgenic mice (c-Fos::tTA/R26R::H2B-mCherry) (*18*). Right, experimental design. (**F**) Freezing levels during tests 1 and 2 (one-way ANOVA). (**G**) Freezing levels during test 3 (one-way ANOVA). (**H**) Representative images showing c-Fos$^+$–mCherry$^+$ overlap in the LA, indicated by arrowheads. Blue, 4′,6-diamidino-2-phenylindole (DAPI) staining. Scale bars, 50 μm. (**I**) c-Fos$^+$–mCherry$^+$ overlap cell counts (one-way ANOVA; $n = 4$ mice per group). Yellow lines represent chance level for each group. *$P < 0.05$; **$P < 0.01$. Data are represented as mean ± SEM.

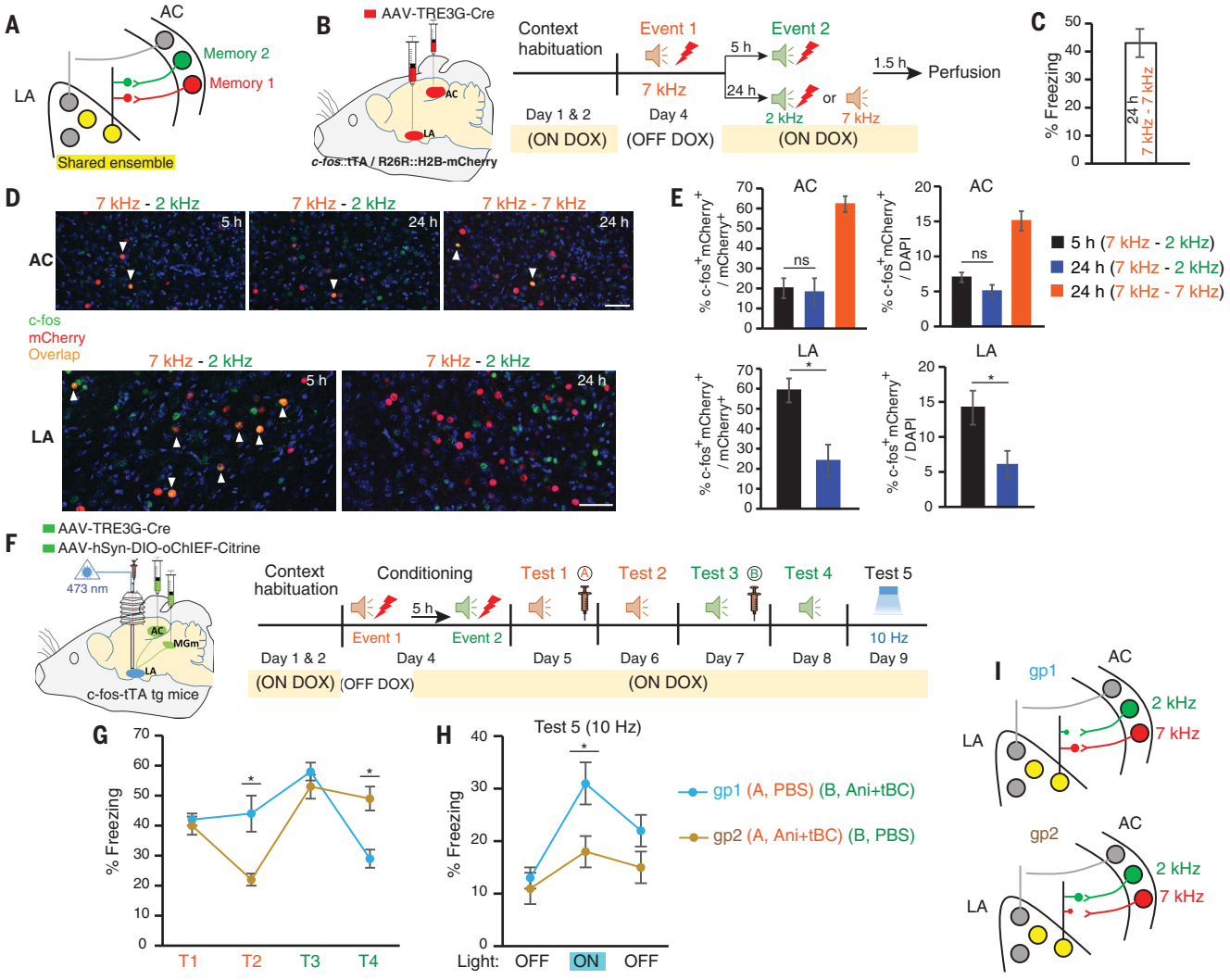

Fig. 3. Synapse-specific erasure of overlapping fear memories. (**A**) Model for the neuronal ensemble in the LA and AC after two associative memories encoded with a 5-hour interval. Memories 1 and 2 respectively correspond to events 1 and 2. (**B**) Left, strategy to label engram cells in the AC and LA using double transgenic mice (c-Fos::tTA/R26R::H2B-mCherry) injected with AAV-TRE$_{3G}$-Cre. Right, experimental design to check the overlapping ensembles between two associative memories that were encoded with different time intervals separating them. (**C**) Freezing level during the 7-kHz test session in the 7-kHz–7-kHz group. (**D**) Top, images for the overlapping ensembles, indicated by arrowheads, in the AC for different time intervals. Bottom, same as top but in the LA. Blue, DAPI staining. Scale bars, 50 μm. (**E**) Top, c-Fos$^+$–mCherry$^+$ overlap cell counts in the AC (one-way ANOVA; n = 4 mice per group). Bottom, same as in top but in the LA (unpaired t test; n = 4 mice per group). (**F**) Design for the selective memory erasure experiment. (**G** and **H**) Freezing levels for gp1 and gp2 during 7- and 2-kHz tones before and after drug injection (G) and during light-off and light-on epochs (H) (unpaired t test; n = 10 mice per group). T1, test 1; T2, test 2; and so forth. (**I**) Model for selective erasure of either 7-kHz-tone fear memory (red) or 2-kHz-tone fear memory (green). Overlapping ensembles are in yellow. *P < 0.05. Data are represented as mean ± SEM.

in event 1 memory–specific synapses (Fig. 4, E and F). Mice that received the LTP protocol displayed higher freezing levels in response to the 7-kHz tone (test 5), whereas freezing responses to the 2-kHz tone (test 6) were unaffected (Fig. 4G).

Storing and distinguishing between several memories encoded in the same neurons are critically important for organizing unique memories. Our findings demonstrate that synapse-specific plasticity is necessary and sufficient for associative fear memory storage and that it guarantees uniqueness to the memory trace, pointing to plasticity as a substrate for the fear memory engram. This perspective is consistent with a recent observation that LTP is selectively induced in specific auditory pathways after fear memory formation (*20*).

Engram cells retain a memory after anisomycin-induced amnesia, and synaptic plasticity is dispensable for memory storage (*21*). However, synaptic plasticity and functional connectivity between engram cell assemblies are indispensable for fear memory storage, because after LTD induction, the depressed synapses might be nonfunctional. Therefore, not only the natural cue, but also the optical stimulation of synapses between the engram cell assemblies failed to retrieve the memory. Furthermore, the engram network no longer retained the associative fear memory after Ani +tBC-induced complete amnesia. The LTP occlusion experiment showed that synaptic potentiation persisted even 2 days after behavioral training in the PBS control group and that complete amnesia accompanied a reset of LTP. This further supports the idea that LTP is important for memory maintenance. The combined evidence suggests that synaptic plasticity can build a specific connectivity within the engram cell assemblies and that the functional connectivity is a simple reflection of the enhanced synaptic strength, rather than an independent mechanism for memory storage.

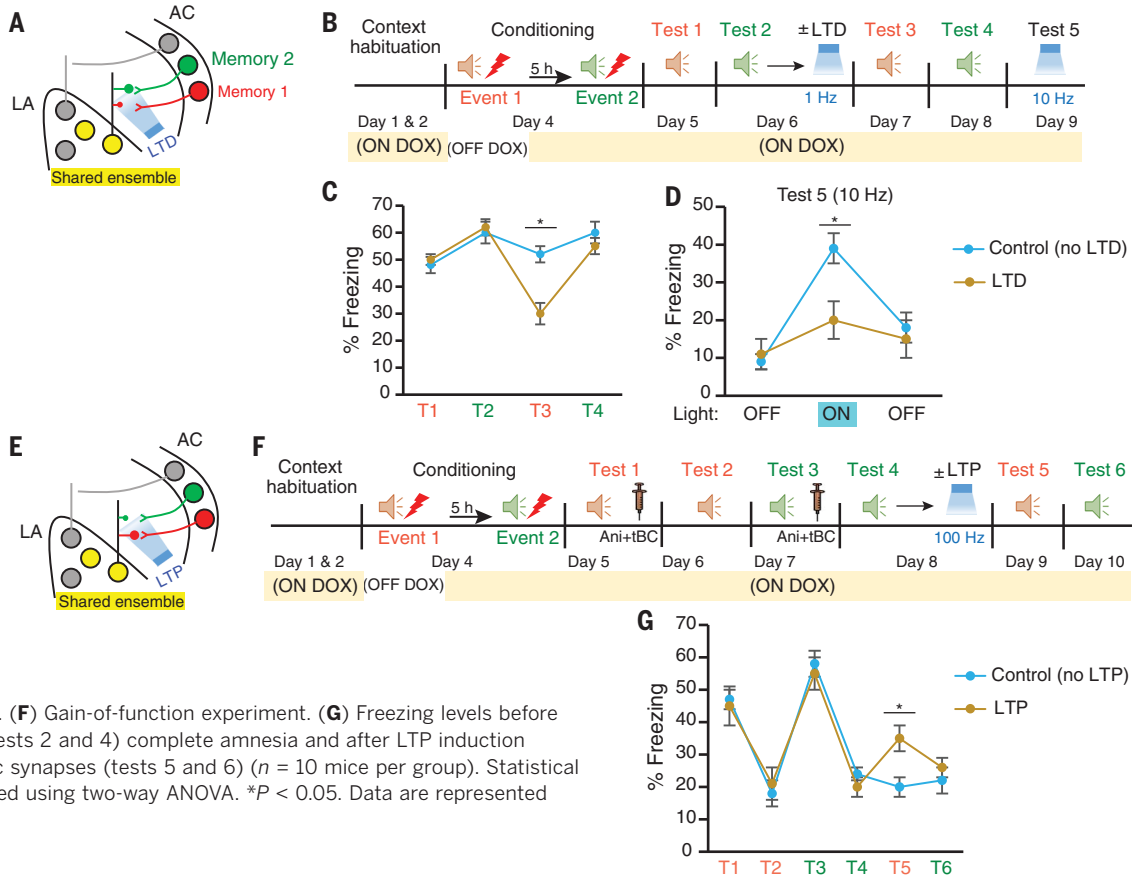

Fig. 4. Engram-specific synaptic plasticity is crucial and sufficient for information storage and keeps the identity of the overlapping memories distinct. (**A**) Model for selective optogenetic targeting of synaptic plasticity with LTD. Memories 1 and 2 respectively correspond to events 1 and 2. (**B**) Design of the loss-of-function experiment. (**C** and **D**) Freezing levels in response to 7- and 2-kHz tones before and after optical LTD induction to event 1 memory–specific synapses (C) and in response to optical stimulation (D) (n = 10 mice per group). (**E**) Model for selective optogenetic targeting of synaptic plasticity with LTP. (**F**) Gain-of-function experiment. (**G**) Freezing levels before (tests 1 and 3) and after (tests 2 and 4) complete amnesia and after LTP induction to event 1 memory–specific synapses (tests 5 and 6) (n = 10 mice per group). Statistical comparisons were performed using two-way ANOVA. *P < 0.05. Data are represented as mean ± SEM.

This study uncovered the mechanism by which the brain can maintain the uniqueness of a massive number of associated memories stored in shared cell ensembles. Furthermore, we achieved selective and total erasure of a fear memory from an engram network without affecting other memories stored in the shared ensemble by resetting the plasticity in a synapse-specific manner. These findings lead to a better understanding of the mechanisms underlying memory storage and may give insight into therapeutic approaches to treating post-traumatic stress disorder.

REFERENCES AND NOTES

1. T. V. Bliss, G. L. Collingridge, *Nature* **361**, 31–39 (1993).
2. T. V. Bliss, T. Lomo, *J. Physiol.* **232**, 331–356 (1973).
3. M. Bocchio, S. Nabavi, M. Capogna, *Neuron* **94**, 731–743 (2017).
4. J. P. Johansen, C. K. Cain, L. E. Ostroff, J. E. LeDoux, *Cell* **147**, 509–524 (2011).
5. S. Nabavi *et al.*, *Nature* **511**, 348–352 (2014).
6. G. Neves, S. F. Cooke, T. V. Bliss, *Nat. Rev. Neurosci.* **9**, 65–75 (2008).
7. S. Tonegawa, M. Pignatelli, D. S. Roy, T. J. Ryan, *Curr. Opin. Neurobiol.* **35**, 101–109 (2015).
8. J. H. Han *et al.*, *Science* **323**, 1492–1496 (2009).
9. S. A. Josselyn, S. Köhler, P. W. Frankland, *Nat. Rev. Neurosci.* **16**, 521–534 (2015).
10. X. Liu *et al.*, *Nature* **484**, 381–385 (2012).
11. L. G. Reijmers, B. L. Perkins, N. Matsuo, M. Mayford, *Science* **317**, 1230–1233 (2007).
12. A. J. Silva, Y. Zhou, T. Rogerson, J. Shobe, J. Balaji, *Science* **326**, 391–395 (2009).
13. S. Tonegawa, X. Liu, S. Ramirez, R. Redondo, *Neuron* **87**, 918–931 (2015).
14. D. J. Cai *et al.*, *Nature* **534**, 115–118 (2016).
15. M. Nomoto *et al.*, *Nat. Commun.* **7**, 12319 (2016).
16. N. Ohkawa *et al.*, *Cell Rep.* **11**, 261–269 (2015).
17. A. J. Rashid *et al.*, *Science* **353**, 383–387 (2016).
18. J. Yokose *et al.*, *Science* **355**, 398–403 (2017).
19. T. Rogerson *et al.*, *Nat. Rev. Neurosci.* **15**, 157–169 (2014).
20. W. B. Kim, J.-H. Cho, *Neuron* **95**, 1129–1146.e5 (2017).
21. T. J. Ryan, D. S. Roy, M. Pignatelli, A. Arons, S. Tonegawa, *Science* **348**, 1007–1013 (2015).
22. P. Tovote, J. P. Fadok, A. Lüthi, *Nat. Rev. Neurosci.* **16**, 317–331 (2015).
23. M. Shehata, K. Inokuchi, *Rev. Neurosci.* **25**, 543–557 (2014).
24. M. Shehata, H. Matsumura, R. Okubo-Suzuki, N. Ohkawa, K. Inokuchi, *J. Neurosci.* **32**, 10413–10422 (2012).
25. M. Shehata *et al.*, *J. Neurosci.* **38**, 3809–3822 (2018).
26. C. C. Huang, C. C. Chen, Y. C. Liang, K. S. Hsu, *Int. J. Neuropsychopharmacol.* **17**, 1233–1242 (2014).
27. S. Park *et al.*, *Sci. Rep.* **6**, 31069 (2016).
28. E. Tsvetkov, W. A. Carlezon Jr., F. M. Benes, E. R. Kandel, V. Y. Bolshakov, *Neuron* **34**, 289–300 (2002).

ACKNOWLEDGMENTS

From the University of Toyama, we thank N. Ohkawa for his help in providing c-Fos::tTA mice, Y. Saitoh and M. Nomoto for their help with electrophysiology, and S. Tsujimura for maintenance of mice. We thank all members of the Inokuchi laboratory for discussion and suggestions. We also thank M. Ito and N. Takino (Jichi Medical University, Japan) for their help with production of the AAV vectors. **Funding:** This work was supported by a Grant-in-Aid for Scientific Research on Innovative Areas ("Memory dynamism"; JP25115002) from the Ministry of Education, Culture, Sports, Science, and Technology of Japan (MEXT); JSPS KAKENHI grant number 23220009; the Core Research for Evolutional Science and Technology (CREST) program (JPMJCR13W1) of the Japan Science and Technology Agency (JST); the Mitsubishi Foundation; the Uehara Memorial Foundation; and the Takeda Science Foundation (to K.I.). Additional support was provided by a Grant-in-Aid for young scientists from JSPS KAKENHI (grant number 25830007) to M.S. The Otsuka Toshimi Scholarship Foundation supported K.A. **Author contributions:** K.A., M.S., and K.I. designed the experiments. K.A., M.S., and K.I. wrote the manuscript. K.A., M.S., and K.C. performed the experiments. K.A., M.S., and K.I. analyzed the data. H.N. and M.M. produced and maintained transgenic mice. S.M. prepared AAVs. **Competing interests:** S.M. owns equity in a company, Gene Therapy Research Institution, that commercializes the use of AAV vectors for gene therapy applications. To the extent that the work in this manuscript increases the value of these commercial holdings, S.M. has a conflict of interest. **Data and materials availability:** All data are available in the main text or the supplementary materials.

SUPPLEMENTARY MATERIALS

www.sciencemag.org/content/360/6394/1227/suppl/DC1
Materials and Methods
Figs. S1 to S7
References (*29*–*31*)

21 February 2018; accepted 26 April 2018
10.1126/science.aat3810

Synapse-specific representation of the identity of overlapping memory engrams

Kareem Abdou, Mohammad Shehata, Kiriko Choko, Hirofumi Nishizono, Mina Matsuo, Shin-ichi Muramatsu and Kaoru Inokuchi

Science **360** (6394), 1227-1231.
DOI: 10.1126/science.aat3810

Disentangling specific memories

Each memory is stored in a distinct memory trace in the brain, in a specific population of neurons called engram cells. How does the brain store and define the identity of a specific memory when two memories interact and are encoded in a shared engram? Abdou *et al.* used optogenetic reactivation coupled with manipulations of long-term potentiation to analyze engrams that share neurons in the lateral amygdala (see the Perspective by Ramirez). Synapse-specific plasticity guaranteed the storage and the identity of individual memories in a shared engram. Moreover, synaptic plasticity between specific engram assemblies was necessary and sufficient for memory engram formation.

Science, this issue p. 1227; see also p. 1182

www.sciencemag.org/content/360/6394/1227/suppl/DC1

Supplementary Materials for

Synapse-specific representation of the identity of overlapping memory engrams

Kareem Abdou*, Mohammad Shehata*, Kiriko Choko, Hirofumi Nishizono, Mina Matsuo, Shin-ichi Muramatsu, Kaoru Inokuchi†

*These authors contributed equally to this work.
†Corresponding author. Email: inokuchi@med.u-toyama.ac.jp

Published 15 June 2018, *Science* **360**, 1227 (2018)
DOI: 10.1126/science.aat3810

This PDF file includes:

Materials and Methods

Animals

Naive male C57BL/6J (purchased from Sankyo Labo Service Co. Inc., Tokyo, Japan) and c-Fos::tTA transgenic mice (Mutant Mouse Regional Resource Center, stock number: 031756-MU) were obtained as described previously (*11*, *16*). The R26R::H2B-mCherry transgenic mice (CDB0204K) have been described previously (*29*). The progeny for the c-Fos::tTA and c-Fos::tTA/R26R::H2B-mCherry double transgenic mouse lines were generated using *in vitro* fertilization with eggs from C57BL/6J mice and embryo transfer techniques. These transgenic mice were raised on food containing 40 mg kg^{-1} DOX and maintained on Dox pellets except for 2 days before the conditioning session. All mice were maintained on a 12 h light/dark cycle at 24°C ± 3°C and 55% ± 5% humidity, had access to food and water *ad libitum*, and were housed with littermates until surgery. Mice for behavioural analyses were 12–18 weeks old. All procedures involving the use of animals were performed in accordance with the guidelines of the National Institutes of Health (NIH) and were approved by the Animal Care and Use Committee of the University of Toyama and the Institutional Committee for the Care and Use of Experimental Animals of Jikei University.

Viral constructs

The recombinant AAV vectors used were AAV-TRE_{3G}-Cre and AAV-hSyn1-DIO-oChIEF-Citrine at a 1:10 ratio. The pAAV-hSyn1-DIO-oChIEF-Citrine plasmid was acquired from Addgene (Addgene plasmid 50973). For pAAV-TRE_{3G}-Cre preparation, pAAV-TRE_{3G}-$CreER^{T2}$ was first constructed by replacement of the PCR-amplified TRE_{3G}-$CreER^{T2}$ of pLenti-TRE_{3G}-$CreER^{T2}$, which has been described previously (*18*), with primers (sense, GCGACGCGTCGAATTCGTCTTCAAGAATTCCTC; antisense, CAGGCCGCGGGAAGGAAG) into pAAV-EF1a-DIO-EYFP (donated by Dr K. Deisseroth) at the *Mlu*I-*Sac*II restriction sites. Then, inverse PCR was performed using the pAAV-TRE_{3G}-$CreER^{T2}$ template with primers (sense, GGATCATCCATCCATCACAGTGGC; antisense, TTAATCGCCATCTTCCAGCAGGCG) to construct pAAV-TRE_{3G}-Cre. The recombinant AAV vectors were produced as described previously (*30*, *31*), and were injected with viral titres of 2.8×10^{13} vg/mL for AAV9-hSyn1-DIO-oChIEF-Citrine and 1.4×10^{13} vg/mL for AAV9-TRE_{3G}-Cre.

Drugs and peptides

Anisomycin (Sigma Aldrich Japan Co., Tokyo, Japan) was dissolved in a minimum quantity of HCl, diluted with phosphate buffered saline (PBS), and adjusted to pH 7.4 with NaOH. The Tat-beclin 1 peptide D-amino acid sequence (RRRQRRKKRGYGGTGFEGDHWIEFTANFVNT; synthesized by GenScript through Funakoshi Co., Ltd., Tokyo, Japan) was dissolved in either PBS (tat-beclin) or anisomycin solution (anisomycin + tat-beclin). Drugs and peptides were aliquoted into single experiment volumes and stored at −80°C.

Surgery

Mice were 10–12 weeks old at the time of surgery. They were anesthetized with isoflurane, given an intraperitoneal injection of pentobarbital solution (80 mg/kg of body weight), and then placed in a stereotactic apparatus (Narishige, Tokyo, Japan). Virus (500 nL) was injected at 100 nL min^{-1} bilaterally into the AC (−2.7 mm anteroposterior [AP], ±4.4 mm mediolateral [ML], +3.3 mm dorsoventral [DV]), MGm (−3.1 mm AP, ±1.9 mm ML, +3.5 mm DV), and LA (−1.7 mm

AP, ±3.4 mm ML, +4.1 mm DV). After injection, the injection cannula was kept in place for 5 min before its withdrawal, then a stainless guide cannula (PlasticsOne, Roanoke, VA, USA) targeting the LA was positioned 3.1 mm ventral to the bregma and fixed on the skull with dental cement. A dummy cannula (PlasticsOne) with a cap was then inserted into the guide cannula. Mice were allowed to recover for at least 7 days in individual home cages before starting the experiments. All drug infusions were performed under isoflurane anaesthesia, using an injection cannula with a 0.25 mm internal diameter (PlasticsOne), and extending beyond the end of the guide cannula by 1 mm. Immediately after retrieval, 0.5 µL of drug solution was injected bilaterally (total: 1 µL/mouse) into the LA at a flow rate of 0.2 µL/min. Following drug infusion, the injection cannula was left for 2 min to allow for drug diffusion. In all experiments, 1 µL of drug solution contained either PBS, 125 µg of anisomycin, or 125 µg of anisomycin + 20 µg of tat-beclin.

Auditory fear conditioning (AFC)

All behavioural sessions were conducted during the light cycle, in a dedicated soundproof behavioural room (Yamaha Co., Shizuoka, Japan), described here as Room A. Different chambers were used for each AFC session. All chambers were different in shape, lighting pattern, and floor texture. After recovery from surgery, a maximum of six mice were moved from their home cages on racks in the maintenance room to a soundproof waiting room (Yamaha Co.). Mice were left undisturbed for at least 15 min before and after each session, and during the experiment. In each session, one mouse in its home cage was moved into Room A. The experiments were performed on AAV-injected c-fos-tTA mice, maintained on food containing 40 mg/kg doxycycline (DOX).

Habituation. Three–four weeks after virus infection, mice were allowed to explore the context for 2 min before exposure to a neutral tone (30 sec, 65 dB, 2 kHz). The mice then remained for an additional 2.5 min before being returned to their home cages. After the second habituation session, DOX was removed and the mice were maintained on normal food. Habituation was done with tone presentation to decrease the startle response to any tone presentation in the subsequent sessions.

Conditioning. Two days later, mice were placed in the context for 2 min, and then received a single presentation of a conditioned tone (30 sec, 65 dB, 7 kHz), co-terminating with a shock (2 sec, 0.4 mA); mice remained for 30 sec, and were then returned to their home cages. Six hours later, the food was changed to one containing 1000 mg/kg DOX.

Testing. Mice were allowed to explore the unfamiliar context for 2 min before receiving the test tone (30 sec, 65 dB, 7 or 2 kHz), then 30 sec later they were returned to their home cages, except in the test 1 condition, where they were subjected to isoflurane anaesthesia and drug infusion.

Optogenetic stimulation (10 and 20 Hz). For the placement of two branch-type optical fibres (internal diameter, 0.25 mm) connected to a housing with a cap, mice were anaesthetized with approximately 2.0% isoflurane and the optic fibres were inserted into guide cannulas. The tip of the optical fibre was targeted 0.5 mm above the LA (DV 3.6 mm from the bregma). Mice with the inserted optic fibres were then returned to their home cages and left for at least 2 h. The fibre unit-connected mouse was attached to an optical swivel, which was connected to a laser unit (8–10 mW, 473 nm). The delivery of light was controlled using a schedule stimulator in time-lapse mode. The optogenetic session was 9 min in duration, and consisted of three 3 min epochs, with the first and third being Light-Off epochs, and the second being a Light-On epoch. During the Light-On epoch, mice received optical stimulation (10 or 20 Hz, 15 ms pulse width) for the entire

3 min. One hour after the end of the session, the fibre was removed from the cannula under anaesthesia.

***In vivo* LTP induction**. Immediately after test 4, mice were placed in a different home cage, and after being allowed 2 min for exploration, optical LTP was induced with 10 trains of light (each train consisted of 100 pulses of light, 5 ms each, at 100 Hz) at 90 sec inter-train intervals.

Experiments consisting of two overlapping memories (Figs. 3, 4, S5 and S6)

Habituation, testing, and optogenetic stimulation sessions were as described above.

Conditioning. After 2 days OFF DOX, mice were fear conditioned to a 7 kHz tone as described above. Immediately after the session, mice were put back on food containing 1000 mg/kg DOX. One hour later, mice were injected intraperitoneally with doxycycline hyclate (120 mg/kg) to stop the expression of oChIEF. Five or twenty-four hours after the 7 kHz fear conditioning, mice were exposed to 2 kHz fear conditioning.

***In vivo* LTP or LTD induction**. Immediately after the test session, optical LTP or LTD was applied. Optical LTP was induced with 10 trains of light (each train consisted of 100 pulses of light, 5 ms each, at 100 Hz) at 90 sec inter-train intervals. Optical LTD was induced with 900 pulses of light, 2 ms each, at 1 Hz.

Two tone discrimination experiment (Fig. S1)

Naive male C57BL/6J mice were used. Mice were exposed to the above-mentioned protocol during the habituation and conditioning sessions. One day after conditioning, mice were divided into two groups, the first of which was tested with the 7 kHz tone first, and was then tested with the 2 kHz tone on the following day, and the second of which was tested with the 2 kHz tone first, and was then tested with the 7 kHz tone. During test sessions, mice were allowed to explore the unfamiliar context for 2 min before receiving the testing tone, and then 30 sec later, the mice were returned to their home cages.

Behavioural analysis

All experiments were conducted using a video tracking system (Muromachi Kikai, Tokyo, Japan) to measure the freezing behaviour of the animals. Freezing was defined as a complete absence of movement, except for respiration. Scoring of the duration of the freezing response was started after 1 sec of sustained freezing behaviour. All behavioural sessions were digitally recorded using Bandicam software (Bandisoft, Seoul, Korea). Animals were excluded when the virus or the cannula was not in the target position.

In vivo LTP or LTD induction (Figs. 1 and 4)

For behavioural experiments, optical LTP was induced with 10 trains of light (each train consisted of 100 pulses of light, 5 ms each, at 100 Hz) at 90 sec inter-train intervals. Optical LTD was induced with 900 pulses of light, 2 ms each, at 1 Hz. For the LTP occlusion experiment, optical LTP was induced with five trains of light (each train consisted of 100 pulses of light, 5 ms each, at 100 Hz) at 3 min inter-train intervals.

In vivo recording (Fig. 2 and S3)

Four weeks after the injection of AAV viral vectors into the MGm and AC, mice were anesthetized with pentobarbital and mounted on a stereotaxic frame. An optic fibre was glued to the recording tungsten electrode so that the tip of the fibre was 500 μm above the tip of the

electrode. The optrode was inserted into the LA, and the optic fibre was connected to a 473 nm laser unit. The LTP or LTD induction protocol was identical to that used in the behavioural test. After establishing a stable baseline at the recording site for 20 min (stimulation frequency of 0.033 Hz), *in vivo* LTP or LTD was optically induced, which was followed by at least 20 min of 0.033 Hz stimulation. Data were analysed using Clampex 10.7 software. All animals were perfused after the recordings, and the positions of the recording sites were verified.

LTP occlusion experiment

The behavioural part of this experiment was performed as described above. One day after the test session and drug infusion, mice were anesthetized and the guide cannulas with dental cement were removed from the skull. *In vivo* recording was then performed as described above.

Immunohistochemistry

One and a half hours after the desired session, the mice were deeply anesthetized with pentobarbital solution and perfused transcardially with PBS (pH 7.4) followed by 4% paraformaldehyde in PBS (PFA). The brains were removed, further post-fixed by immersion in PFA for 12–18 h at 4°C, equilibrated in 25% sucrose in PBS for 36–48 h at 4°C, and then stored at –80°C. Brains were cut into 50 μm coronal sections using a cryostat and transferred to 12-well cell culture plates (Corning, NY, USA) containing PBS. After washing with PBS, the floating sections were treated with blocking buffer (3% normal donkey serum; S30, Chemicon by EMD Millipore, Billerica, MA, USA) in PBS containing 0.2% Triton X-100 and 0.05% tween 20 (PBST), at room temperature for 1 h. The following primary antibodies were applied in blocking buffer at 4°C for 24–36 h: rat anti-GFP (1:1000, Nacalai Tesque, 04404-84, GF090R), rabbit anti-c-Fos (1:1000, Santa Cruz Biotechnology, sc-7202), goat anti-c-Fos (1:1000, Santa Cruz Biotechnology, sc-52-G), and rabbit anti-mCherry (1:1000, Clontech, 632496). After three 10 min washes with 0.2% PBST, sections were incubated in blocking buffer at room temperature for 2–3 h, with the following corresponding secondary antibodies: donkey anti-rat IgG Alexa Fluor 488 (1:1000, Molecular Probes, A21208), donkey anti-rabbit IgG Alexa Fluor 546 (1:1000, Molecular Probes, A10040), or donkey anti-goat IgG Alexa Fluor 647 (1:1000, Molecular Probes, A21447). Finally, the sections were treated with DAPI (1 μg/mL, Roche Diagnostics, 10236276001) and then washed with 0.2% PBST three times for 10 min each before being mounted onto glass slides with ProLong Gold antifade reagent (Invitrogen).

Confocal microscopy and cell counting

Images were acquired using a Zeiss LSM 780 confocal microscope (Carl Zeiss, Jena, Germany) with a 20× plan apochromat objective lens. All acquisition parameters were kept constant within each magnification. To quantify the number of each immunoreactive cell type in the target regions after collecting z-stacks (approximately 10 optical sections of 10 μm thickness), three coronal sections per mouse (n = 4 mice) were manually counted. Overlaps between the GFP^+ and $c\text{-}fos^+$ cells, as well as $mCherry^+$ and $c\text{-}fos^+$ cells, were manually counted. Chance level was calculated by multiplying % $mCherry^+$ / DAPI by % $c\text{-}fos^+$ / DAPI.

Statistics

Statistical analyses were performed using Prism 6.01 (GraphPad Software, San Diego, CA, USA). Data from two groups were compared using two-tailed unpaired Student's *t*-tests. Multiple-

group comparisons were assessed using ANOVA with post hoc tests as described in the appropriate figure legend. Quantitative data are presented as mean ± s.e.m.

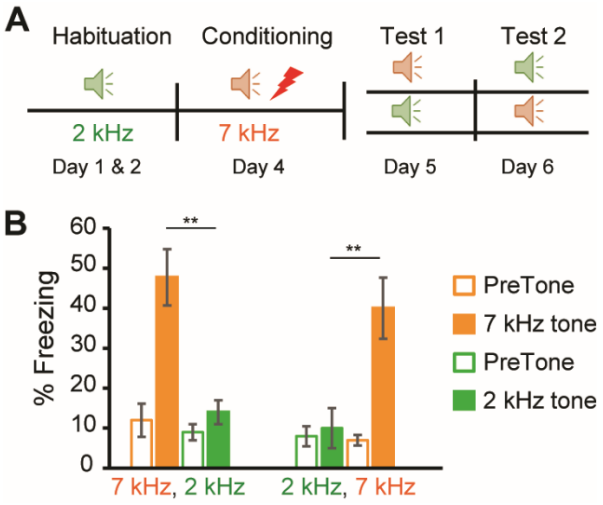

Fig. S1. Mice discriminate between 2 kHz and 7 kHz tones.

(**A**) Design for the discrimination experiment. Wild-type mice were exposed to AFC and then divided into two groups; the first one received a 7 kHz tone in test 1 and a 2 kHz tone in test 2, while the second group received the tones in the opposite order. (**B**) Freezing levels before and during the two tones (n = 11 mice/group). Statistical comparisons were performed using a paired t-test. * $P < 0.05$; ** $P < 0.01$. Data are represented as mean ± SEM.

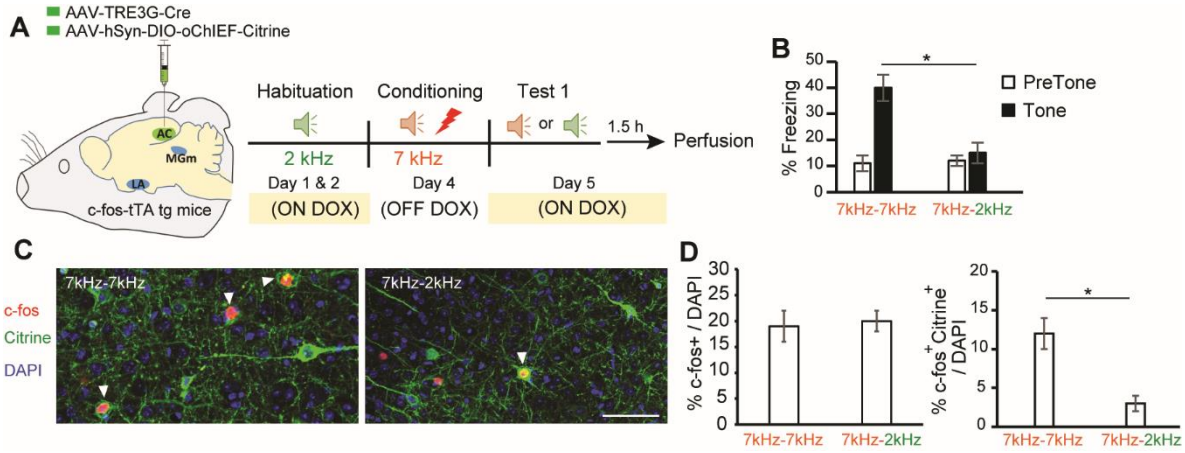

Fig. S2. 7 kHz and 2 kHz tones activate different neuronal ensembles in the AC.

(**A**) Experimental design to label the 7 kHz and 2 kHz-responsive ensembles in the AC with citrine and c-Fos antibodies, respectively. (**B**) Freezing levels before and during 7 kHz and 2 kHz tone presentations in test sessions. (**C**) Representative images showing two different ensembles encoding different tones. Arrow heads represent overlapping cells (c-Fos$^+$/citrine$^+$ overlap). Scale bars, 50 μm. (**D**) Left, c-Fos$^+$ neurons activated during test session. Right, c-Fos$^+$/citrine$^+$ overlap cell counts (n = 4 mice/group). Statistical comparisons were performed using an unpaired t-test. * $P < 0.05$. Data are represented as mean ± SEM.

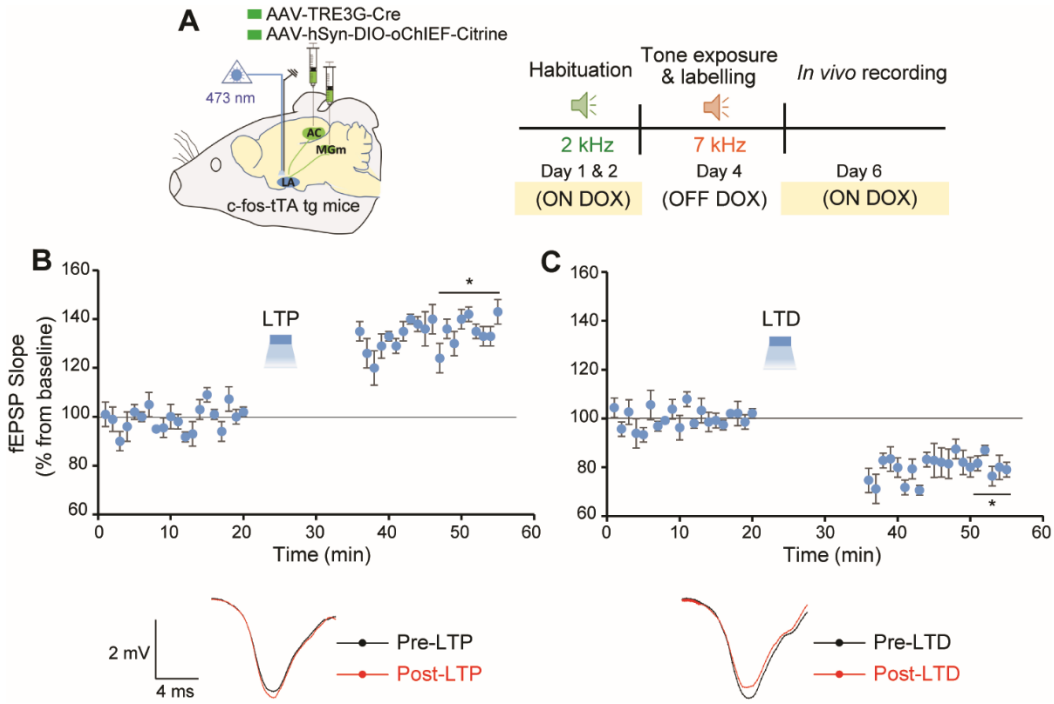

Fig. S3. *In vivo* induction of optical LTP and LTD.

(**A**) Experimental design. (**B**) Top, average of *in vivo* field EPSP slope (normalized to baseline) before and after LTP induction (n = 4 mice/group). Bottom, representative traces before (black) and after (red) the stimulation protocol. (**C**) Top, average of *in vivo* field EPSP slope (normalized to baseline) before and after LTD induction (n = 4 mice/group). Bottom, representative traces before (black) and after (red) the stimulation protocol. Statistical comparisons were performed using two-way repeated measures ANOVA. * $P < 0.05$. Data are represented as mean ± SEM.

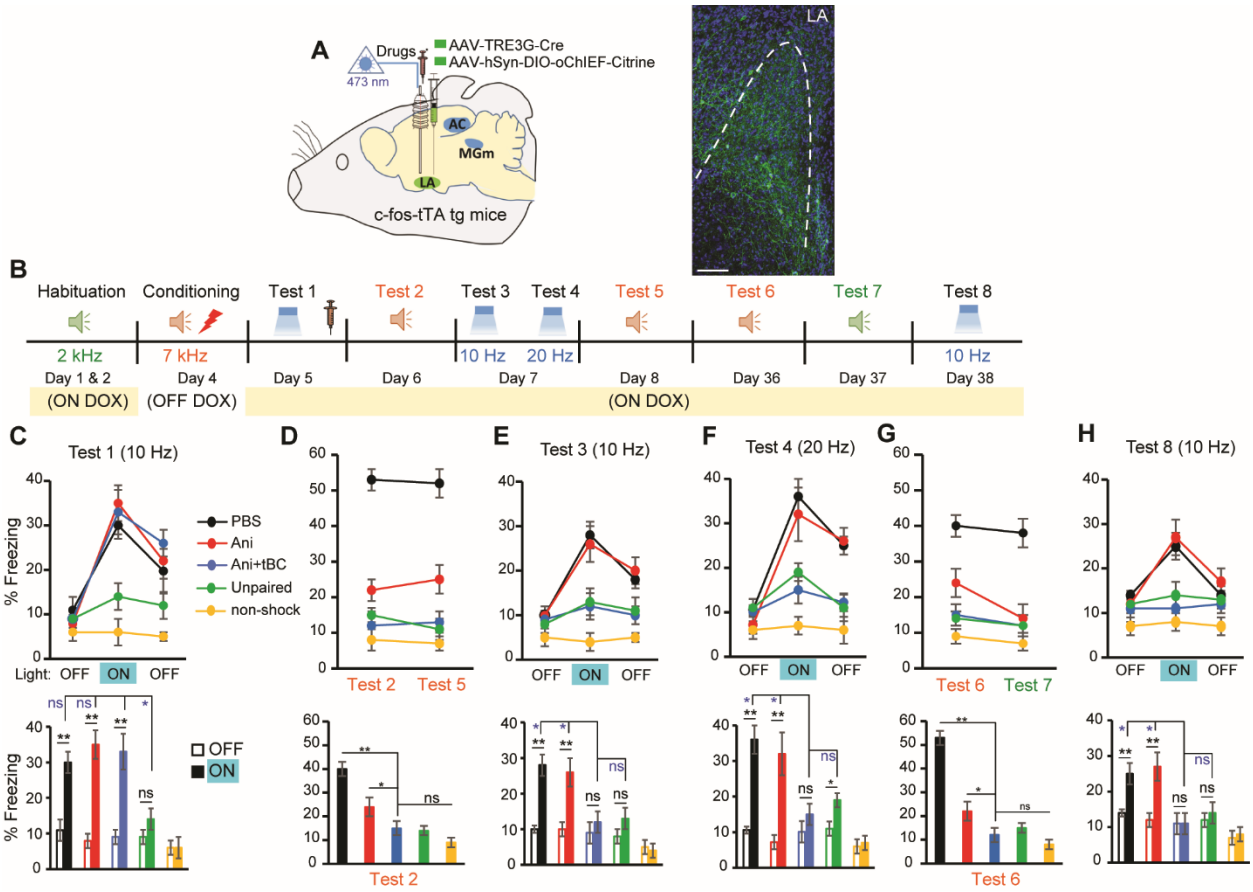

Fig. S4. LA engram cells no longer store the memory after complete amnesia.

(**A**) Left, labelling strategy for the AFC-responsive ensemble in LA using the c-Fos/TetTag system. Right, expression of oChIEF in LA neurons. Dashed line shows the border of LA. Scale bar, 100 μm. (**B**) Experimental design for erasure of the memory engram. (**C** to **H**) Top, freezing levels during fear memory recall by 10 Hz stimulation (**C**), in response to the conditioned tone (**D**), during 10 Hz stimulation (**E**), during 20 Hz stimulation (**F**), in response to the conditioned tone and neutral tone at a remote time point (**G**), and during 10 Hz stimulation at a remote time point (**H**). Bottom, statistical significance between groups (n = 10 mice/group). Statistical comparisons were performed using one-way ANOVA (**D** and **G**) and two-way ANOVA (**C**, **E**, **F** and **H**). Ani, anisomycin; tBC, tat-beclin. * $P < 0.05$; ** $P < 0.01$. Data are represented as mean ± SEM.

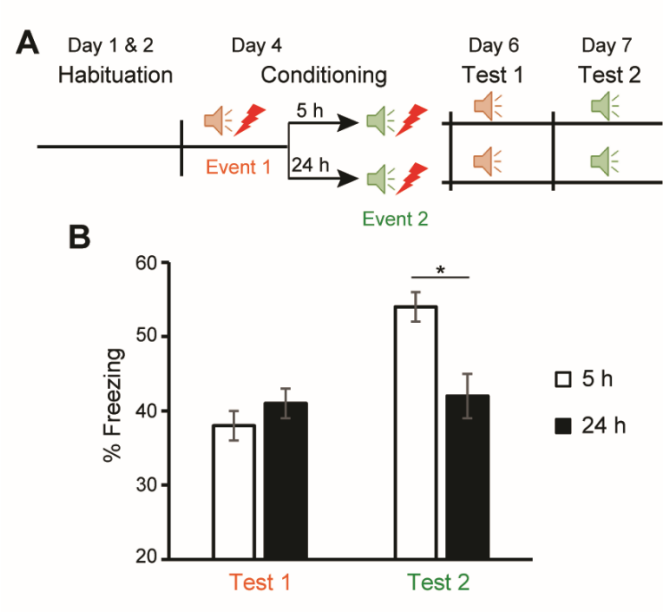

Fig. S5. Memory enhancement after encoding two memories 5 hours apart.

(**A**) Design for the memory linking experiment. Wild-type mice were exposed to event 1 (7 kHz + shock) and then divided into two groups. The first group was exposed to event 2 (2 kHz + shock) 5 h after being exposed to event 1, while the second group was exposed to event 2 after 24 h. Both groups received a 7 kHz tone in test 1, while they received a 2 kHz tone in test 2. (**B**) Freezing levels of both groups in tests 1 and 2 ($n = 6$ mice/group). Statistical comparisons were performed using an unpaired *t*-test. * $P < 0.05$. Data are represented as mean ± SEM.

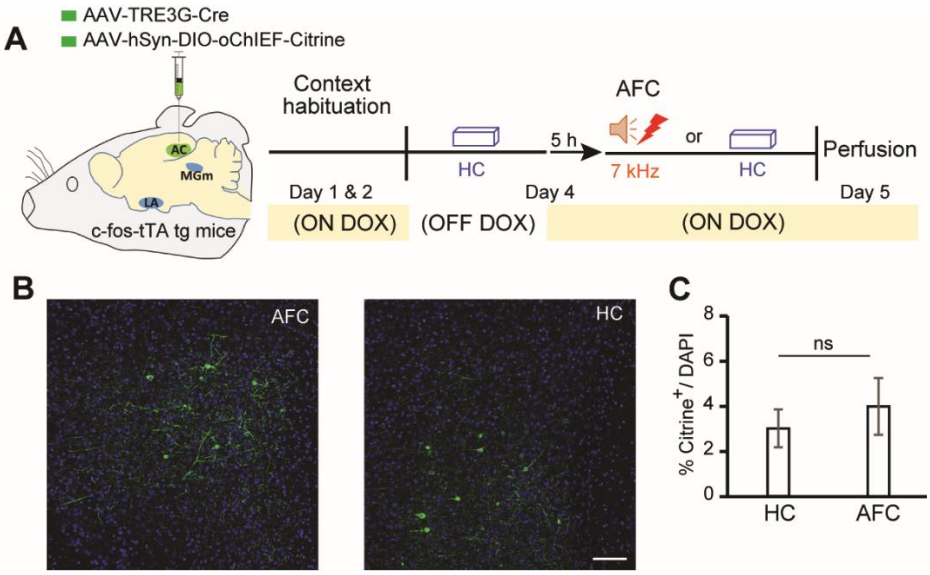

Fig. S6. Five hours ON DOX is enough to stop the expression of oChIEF.

(**A**) Experimental design. After 2 days without DOX in their food, mice were put back on DOX for 5 h, and were then either exposed to AFC or stayed in their home cage (HC). One day later, they were perfused. (**B**) Representative images showing oChIEF-citrine expression in AC after AFC while mice were ON DOX chow (1 g kg^{-1}). Scale bar, 100 µm. (**C**) oChIEF-citrine cell counts (unpaired *t*-test, $n = 4$ mice/group). * $P < 0.05$. Data are represented as mean ± SEM.

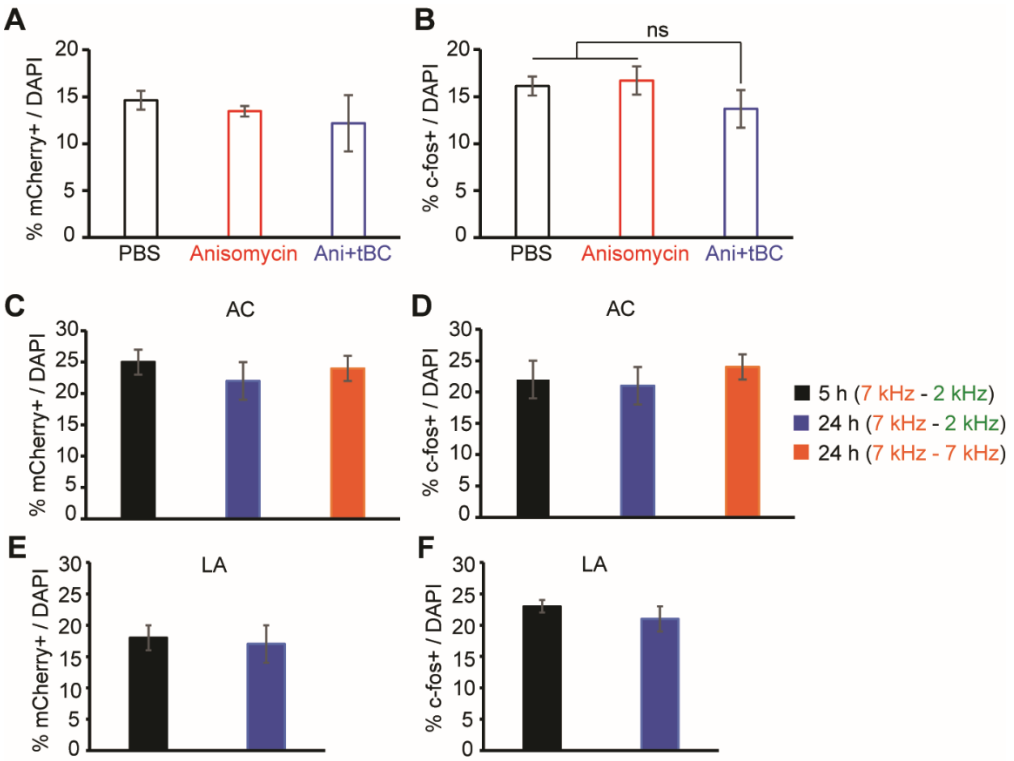

Fig. S7. Efficiency of engram labelling was similar across groups.

(**A** and **B**) Related to figure 2, E to I. (**A**) Counts for mCherry^{+} neurons which activated during 7 kHz fear conditioning. (**B**) Counts for c-Fos^{+} neurons which activated in response to 10Hz optogenetic stimulation. (**C** to **F**) Related to figure 3, A to E. (**C** and **E**) Counts for mCherry^{+} neurons which activated during 7 kHz fear conditioning in AC (**C**) and in LA (**E**). (**D** and **F**) Counts for c-Fos+ neurons in AC (**D**) and in LA (**F**). Data are represented as mean ± SEM.

References and Notes

1. T. V. Bliss, G. L. Collingridge, A synaptic model of memory: Long-term potentiation in the hippocampus. *Nature* **361**, 31–39 (1993). doi:10.1038/361031a0 Medline

2. T. V. Bliss, T. Lomo, Long-lasting potentiation of synaptic transmission in the dentate area of the anaesthetized rabbit following stimulation of the perforant path. *J. Physiol.* **232**, 331–356 (1973). doi:10.1113/jphysiol.1973.sp010273 Medline

3. M. Bocchio, S. Nabavi, M. Capogna, Synaptic Plasticity, Engrams, and Network Oscillations in Amygdala Circuits for Storage and Retrieval of Emotional Memories. *Neuron* **94**, 731–743 (2017). doi:10.1016/j.neuron.2017.03.022 Medline

4. J. P. Johansen, C. K. Cain, L. E. Ostroff, J. E. LeDoux, Molecular mechanisms of fear learning and memory. *Cell* **147**, 509–524 (2011). doi:10.1016/j.cell.2011.10.009 Medline

5. S. Nabavi, R. Fox, C. D. Proulx, J. Y. Lin, R. Y. Tsien, R. Malinow, Engineering a memory with LTD and LTP. *Nature* **511**, 348–352 (2014). doi:10.1038/nature13294 Medline

6. G. Neves, S. F. Cooke, T. V. Bliss, Synaptic plasticity, memory and the hippocampus: A neural network approach to causality. *Nat. Rev. Neurosci.* **9**, 65–75 (2008). doi:10.1038/nrn2303 Medline

7. S. Tonegawa, M. Pignatelli, D. S. Roy, T. J. Ryan, Memory engram storage and retrieval. *Curr. Opin. Neurobiol.* **35**, 101–109 (2015). doi:10.1016/j.conb.2015.07.009 Medline

8. J. H. Han, S. A. Kushner, A. P. Yiu, H.-L. Hsiang, T. Buch, A. Waisman, B. Bontempi, R. L. Neve, P. W. Frankland, S. A. Josselyn, Selective erasure of a fear memory. *Science* **323**, 1492–1496 (2009). doi:10.1126/science.1164139 Medline

9. S. A. Josselyn, S. Köhler, P. W. Frankland, Finding the engram. *Nat. Rev. Neurosci.* **16**, 521–534 (2015). doi:10.1038/nrn4000 Medline

10. X. Liu, S. Ramirez, P. T. Pang, C. B. Puryear, A. Govindarajan, K. Deisseroth, S. Tonegawa, Optogenetic stimulation of a hippocampal engram activates fear memory recall. *Nature* **484**, 381–385 (2012). Medline

11. L. G. Reijmers, B. L. Perkins, N. Matsuo, M. Mayford, Localization of a stable neural correlate of associative memory. *Science* **317**, 1230–1233 (2007). doi:10.1126/science.1143839 Medline

12. A. J. Silva, Y. Zhou, T. Rogerson, J. Shobe, J. Balaji, Molecular and cellular approaches to memory allocation in neural circuits. *Science* **326**, 391–395 (2009). doi:10.1126/science.1174519 Medline

13. S. Tonegawa, X. Liu, S. Ramirez, R. Redondo, Memory Engram Cells Have Come of Age. *Neuron* **87**, 918–931 (2015). doi:10.1016/j.neuron.2015.08.002 Medline

14. D. J. Cai, D. Aharoni, T. Shuman, J. Shobe, J. Biane, W. Song, B. Wei, M. Veshkini, M. La-Vu, J. Lou, S. E. Flores, I. Kim, Y. Sano, M. Zhou, K. Baumgaertel, A. Lavi, M. Kamata, M. Tuszynski, M. Mayford, P. Golshani, A. J. Silva, A shared neural ensemble links distinct contextual memories encoded close in time. *Nature* **534**, 115–118 (2016). doi:10.1038/nature17955 Medline

15. M. Nomoto, N. Ohkawa, H. Nishizono, J. Yokose, A. Suzuki, M. Matsuo, S. Tsujimura, Y. Takahashi, M. Nagase, A. M. Watabe, F. Kato, K. Inokuchi, Cellular tagging as a neural network mechanism for behavioural tagging. *Nat. Commun.* **7**, 12319 (2016). doi:10.1038/ncomms12319 Medline

16. N. Ohkawa, Y. Saitoh, A. Suzuki, S. Tsujimura, E. Murayama, S. Kosugi, H. Nishizono, M. Matsuo, Y. Takahashi, M. Nagase, Y. K. Sugimura, A. M. Watabe, F. Kato, K. Inokuchi, Artificial association of pre-stored information to generate a qualitatively new memory. *Cell Rep.* **11**, 261–269 (2015). doi:10.1016/j.celrep.2015.03.017 Medline

17. A. J. Rashid, C. Yan, V. Mercaldo, H.-L. Hsiang, S. Park, C. J. Cole, A. De Cristofaro, J. Yu, C. Ramakrishnan, S. Y. Lee, K. Deisseroth, P. W. Frankland, S. A. Josselyn, Competition between engrams influences fear memory formation and recall. *Science* **353**, 383–387 (2016). doi:10.1126/science.aaf0594 Medline

18. J. Yokose, R. Okubo-Suzuki, M. Nomoto, N. Ohkawa, H. Nishizono, A. Suzuki, M. Matsuo, S. Tsujimura, Y. Takahashi, M. Nagase, A. M. Watabe, M. Sasahara, F. Kato, K. Inokuchi, Overlapping memory trace indispensable for linking, but not recalling, individual memories. *Science* **355**, 398–403 (2017). doi:10.1126/science.aal2690 Medline

19. T. Rogerson, D. J. Cai, A. Frank, Y. Sano, J. Shobe, M. F. Lopez-Aranda, A. J. Silva, Synaptic tagging during memory allocation. *Nat. Rev. Neurosci.* **15**, 157–169 (2014). doi:10.1038/nrn3667 Medline

20. W. B. Kim, J.-H. Cho, Encoding of Discriminative Fear Memory by Input-Specific LTP in the Amygdala. *Neuron* **95**, 1129–1146.e5 (2017). doi:10.1016/j.neuron.2017.08.004 Medline

21. T. J. Ryan, D. S. Roy, M. Pignatelli, A. Arons, S. Tonegawa, Engram cells retain memory under retrograde amnesia. *Science* **348**, 1007–1013 (2015). doi:10.1126/science.aaa5542 Medline

22. P. Tovote, J. P. Fadok, A. Lüthi, Neuronal circuits for fear and anxiety. *Nat. Rev. Neurosci.* **16**, 317–331 (2015). doi:10.1038/nrn3945 Medline

23. M. Shehata, K. Inokuchi, Does autophagy work in synaptic plasticity and memory? *Rev. Neurosci.* **25**, 543–557 (2014). doi:10.1515/revneuro-2014-0002 Medline

24. M. Shehata, H. Matsumura, R. Okubo-Suzuki, N. Ohkawa, K. Inokuchi, Neuronal stimulation induces autophagy in hippocampal neurons that is involved in AMPA receptor degradation after chemical long-term depression. *J. Neurosci.* **32**, 10413–10422 (2012). doi:10.1523/JNEUROSCI.4533-11.2012 Medline

25. M. Shehata, K. Abdou, K. Choko, M. Matsuo, H. Nishizono, K. Inokuchi, Autophagy enhances memory erasure through synaptic destabilization. *J. Neurosci.* **38**, 3809–3822 (2018). doi:10.1523/JNEUROSCI.3505-17.2018 Medline

26. C. C. Huang, C. C. Chen, Y. C. Liang, K. S. Hsu, Long-term potentiation at excitatory synaptic inputs to the intercalated cell masses of the amygdala. *Int. J. Neuropsychopharmacol.* **17**, 1233–1242 (2014). doi:10.1017/S1461145714000133 Medline

27. S. Park, J. Lee, K. Park, J. Kim, B. Song, I. Hong, J. Kim, S. Lee, S. Choi, Sound tuning of amygdala plasticity in auditory fear conditioning. *Sci. Rep.* **6**, 31069 (2016). doi:10.1038/srep31069 Medline

28. E. Tsvetkov, W. A. Carlezon Jr., F. M. Benes, E. R. Kandel, V. Y. Bolshakov, Fear conditioning occludes LTP-induced presynaptic enhancement of synaptic transmission in the cortical pathway to the lateral amygdala. *Neuron* **34**, 289–300 (2002). doi:10.1016/S0896-6273(02)00645-1 Medline

29. T. Abe, H. Kiyonari, G. Shioi, K. Inoue, K. Nakao, S. Aizawa, T. Fujimori, Establishment of conditional reporter mouse lines at ROSA26 locus for live cell imaging. *Genesis* **49**, 579–590 (2011). doi:10.1002/dvg.20753 Medline

30. A. Iida, N. Takino, H. Miyauchi, K. Shimazaki, S. Muramatsu, Systemic delivery of tyrosine-mutant AAV vectors results in robust transduction of neurons in adult mice. *BioMed Res. Int.* **2013**, 974819 (2013). doi:10.1155/2013/974819 Medline

31. X. G. Li, T. Okada, M. Kodera, Y. Nara, N. Takino, C. Muramatsu, K. Ikeguchi, F. Urano, H. Ichinose, D. Metzger, P. Chambon, I. Nakano, K. Ozawa, S. Muramatsu, Viral-mediated temporally controlled dopamine production in a rat model of Parkinson disease. *Mol. Ther.* **13**, 160–166 (2006). doi:10.1016/j.ymthe.2005.08.009 Medline